Generating a four-photon polarization-entangled cluster state with homodyne measurement via cross-Kerr nonlinearity*

Su Shi-Lei(苏石磊), Wang Yuan(王 媛), Guo Qi(郭 奇),
Wang Hong-Fu(王洪福), and Zhang Shou(张 寿)†

Department of Physics, College of Science, Yanbian University, Yanji 133002, *China*

(Received 20 July 2011; revised manuscript received 10 September 2011)

We propose a protocol to generate a four-photon polarization-entangled cluster state with cross-Kerr nonlinearity by using the interference of polarized photons. The protocol is based on optical elements, cross-Kerr nonlinearity, and homodyne measurement, therefore it is feasible with current experimental technology. The success probability of our protocol is optimal, this property makes our protocol more efficient than others in the applications of quantum communication.

Keywords: cluster state, homodyne measurement, cross-Kerr nonlinearity

PACS: 42.50.–p, 03.67.–a, 42.65.–k **DOI:** 10.1088/1674-1056/21/4/044205

1. Introduction

The study of two or multi-particles' entanglement, whose joint states cannot be written in a product form,[1] has been a key ingredient of quantum information theory and seems to be crucial to achieve tasks of quantum information processing, such as quantum cryptography,[2] quantum dense coding,[3] and quantum teleportation.[4] As a special entangled state, the four-particle cluster state,

$$|\text{cluster}\rangle = \frac{1}{2}(|0\rangle_1|0\rangle_2|0\rangle_3|0\rangle_4 + |0\rangle_1|0\rangle_2|1\rangle_3|1\rangle_4 + |1\rangle_1|1\rangle_2|0\rangle_3|0\rangle_4 - |1\rangle_1|1\rangle_2|1\rangle_3|1\rangle_4), \quad (1)$$

which was first introduced by Briegel *et al.*,[5] can be regarded as a resource for the so-called one-way quantum computation scheme,[6,7] Greenberger–Horne–Zeilinger (GHZ) state preparation, and is more immune against decoherence than GHZ states.[8] Because of the fact that cluster states have been shown to constitute a universal resource for quantum computation assisted by local measurement only,[9] the cluster states have attracted more attention in theoretical research and practical applications.[10−14] In Ref. [15], Zou *et al.* proposed a scheme to generate a four-photon polarization-entangled cluster state with a success probability 1/4 in an ideal case. On this basis, we propose a modified protocol to generate a four-photon polarization-entangled cluster state with a higher success probability by using cross-Kerr nonlinearity, ancillary coherent states, momentum homodyne measurement, and appropriate unitary operations. Before introducing the structure of this paper, let us first become acquainted with the effect of the cross-Kerr nonlinearity. The Hamiltonian of the cross-Kerr nonlinearity is[16−19]

$$\hat{H}_K = \hbar\chi\hat{n}_a\hat{n}_c, \quad (2)$$

where $\hat{n}_a$ and $\hat{n}_c$ are the photon number operators for modes a and c, respectively. χ is the coupling strength of the nonlinearity, which is determined by the property of the nonlinear material. For example, a coherent beam in the state $|\alpha\rangle$ with a single pulse in the Fock state $|\varphi\rangle = a|0\rangle + b|1\rangle$, we note that $|0\rangle$ and $|1\rangle$ are not the polarization of the photons, but the number of the photons, after the interaction with the cross-Kerr nonlinear medium, evolves as

$$U_K|\varphi\rangle|\alpha\rangle = \mathrm{e}^{\mathrm{i}H_K t/\hbar}(a|0\rangle + b|1\rangle)|\alpha\rangle = a|0\rangle|\alpha\rangle + b|1\rangle|\alpha\,\mathrm{e}^{\mathrm{i}\theta}\rangle, \quad (3)$$

where $\theta = \chi t$, and t is the interaction time. It is clear that the phase shift on the coherent state is directly proportional to the number of photons in signal mode

*Project supported by the National Natural Science Foundation of China (Grant Nos. 61068001 and 11064016).
†Corresponding author. E-mail: szhang@ybu.edu.cn
© 2012 Chinese Physical Society and IOP Publishing Ltd

a and that the Fock state is unaffected. So the measurement on the phase of probe beam can distinguish the photon numbers in signal mode.

The structure of our paper is as follows: In Section 2, we briefly review Zou and coworker's protocol[15] and use the similar method to generate the four-photon polarization-entangled cluster state. But compared with their protocol, the present protocol uses cross-Kerr nonlinearity and homodyne measurement rather than photon detectors in the protocol in Ref. [15]. We can distinguish the bunching outcomes from unbunching ones with different phase shifts by homodyne–heterodyne measurements.[20−22] The state corresponding to unbunching outcomes is the cluster state that we want to generate. In Section 3, we adopt countermeasures to change bunching outcomes to unbunching ones, in other words, the success probability could be improved, which is crucial in our protocol. We can predict whether the protocol is successful or not according to the results of the homodyne measurement. In Section 4, we discuss the influence of the error and give a conclusion.

2. Preparation of the four-photon polarization-entangled cluster state

In the following we propose our protocol to generate the four-photon polarization-entangled cluster state. For the sake of clarity, let us first review Zou and coworker's protocol. By employing the two-photon polarization entangled states $|\Psi\rangle_{\rm EPR} = (|H\rangle_1|H\rangle_2 + |V\rangle_1|V\rangle_2)/\sqrt{2}$, and two single-photon sources: $|\Psi\rangle_3 = |H\rangle_3$, $|\Psi\rangle_4 = |H\rangle_4$, they proposed an encoding circuit to realize the transformation

$$\begin{aligned}&\frac{1}{\sqrt{2}}(|H\rangle_1|H\rangle_2+|V\rangle_1|V\rangle_2)|H\rangle_3|H\rangle_4\\ \longrightarrow\ &\frac{1}{2}(|H\rangle_a|H\rangle_b|H\rangle_c|H\rangle_d+|H\rangle_a|H\rangle_b|V\rangle_c|V\rangle_d\\ &+|V\rangle_a|V\rangle_b|H\rangle_c|H\rangle_d-|V\rangle_a|V\rangle_b|V\rangle_c|V\rangle_d),\end{aligned}\tag{4}$$

with the help of coincidence detection, where H and V denote horizontal and vertical linear polarizations respectively, and the subscript i $(i = 1, 2, 3, 4, a, b, c, d)$ denotes the spatial mode of photons. Their success probability to obtain a cluster state is 1/4 in an ideal condition.

We now present a detailed analysis of our protocol. The schematic diagram of Section 2 of our protocol is shown in Fig. 1, which requires two single-photon states and one two-photon polarization state as input resources and consists of two polarization beam splitters PBS_i $(i = 1, 2)$, three half wave plates HWP_i $(i = 1, 2, 3)$, one ancillary coherent state $|\alpha\rangle_1$, and two cross-Kerr nonlinearity media. We suppose the EPR denotes the state $|\psi\rangle = (|H\rangle_1|H\rangle_2 + |V\rangle_1|V\rangle_2)/\sqrt{2}$, these single-photon input states in modes 3 and 4 are horizontally polarized. So the total input state of the whole system is

$$|\Psi\rangle_0 = \frac{1}{\sqrt{2}}(|H\rangle_1|H\rangle_2+|V\rangle_1|V\rangle_2)|H\rangle_3|H\rangle_4|\alpha\rangle_1.\tag{5}$$

After passing the device in Fig. 1, equation (5) transforms into

$$\begin{aligned}|\Psi\rangle_1 = \frac{1}{4}[&(|H\rangle_a|H\rangle_b|H\rangle_c|H\rangle_d+|H\rangle_a|H\rangle_b|V\rangle_c|V\rangle_d\\ &+|V\rangle_a|V\rangle_b|H\rangle_c|H\rangle_d\\ &-|V\rangle_a|V\rangle_b|V\rangle_c|V\rangle_d)|\alpha\,\mathrm{e}^{4\mathrm{i}\theta_1}\rangle_1\\ &+(|H\rangle_a|H\rangle_b|H\rangle_c|V\rangle_c\\ &+|V\rangle_a|V\rangle_b|H\rangle_c|V\rangle_c)|\alpha\,\mathrm{e}^{7\mathrm{i}\theta_1}\rangle_1\\ &+(|H\rangle_a|V\rangle_a|H\rangle_c|H\rangle_d\\ &+|H\rangle_a|V\rangle_a|V\rangle_c|V\rangle_d)|\alpha\,\mathrm{e}^{5\mathrm{i}\theta_1}\rangle_1\\ &+(|H\rangle_a|H\rangle_b|H\rangle_d|V\rangle_d\\ &-|V\rangle_a|V\rangle_b|H\rangle_d|V\rangle_d)|\alpha\,\mathrm{e}^{\mathrm{i}\theta_1}\rangle_1\\ &+(|H\rangle_b|V\rangle_b|H\rangle_c|H\rangle_d\\ &-|H\rangle_b|V\rangle_b|V\rangle_c|V\rangle_d)|\alpha\,\mathrm{e}^{3\mathrm{i}\theta_1}\rangle_1\\ &+|H\rangle_a|V\rangle_a|H\rangle_c|V\rangle_c|\alpha\,\mathrm{e}^{8\mathrm{i}\theta_1}\rangle_1\\ &+|H\rangle_a|V\rangle_a|H\rangle_d|V\rangle_d|\alpha\,\mathrm{e}^{2\mathrm{i}\theta_1}\rangle_1\\ &+|H\rangle_b|V\rangle_b|H\rangle_c|V\rangle_c|\alpha\,\mathrm{e}^{6\mathrm{i}\theta_1}\rangle_1\\ &-|H\rangle_b|V\rangle_b|H\rangle_d|V\rangle_d|\alpha\rangle_1].\end{aligned}\tag{6}$$

In Eq. (6), for convenience, we have quoted some notations and results in Ref. [15], then, we choose momentum quadrature homodyne measurements on mode 5. For the convenience of analysis, we expand the state in terms of the eigenstates of the $\hat{p}$ operator[23]

$$|\Psi\rangle_1 = \int |p\rangle\langle p|\Psi\rangle_1\,\mathrm{d}p,\tag{7}$$

$$\begin{aligned}|\Psi\rangle_p &= \langle p|\Psi\rangle_1\\ &= N(g_0\,\mathrm{e}^{\mathrm{i}\tau_0}|\varphi\rangle_0+\sqrt{2}g_1\,\mathrm{e}^{\mathrm{i}\tau_1}|\varphi\rangle_1\\ &\quad+g_2\,\mathrm{e}^{\mathrm{i}\tau_2}|\varphi\rangle_2+\sqrt{2}g_3\,\mathrm{e}^{\mathrm{i}\tau_3}|\varphi\rangle_3+2g_4\,\mathrm{e}^{\mathrm{i}\tau_4}|\varphi\rangle_4\\ &\quad+\sqrt{2}g_5\,\mathrm{e}^{\mathrm{i}\tau_5}|\varphi\rangle_5+g_6\,\mathrm{e}^{\mathrm{i}\tau_6}|\varphi\rangle_6\\ &\quad+\sqrt{2}g_7\,\mathrm{e}^{\mathrm{i}\tau_7}|\varphi\rangle_7+g_8\,\mathrm{e}^{\mathrm{i}\tau_8}|\varphi\rangle_8),\end{aligned}\tag{8}$$

where

$$|\varphi\rangle_0 = -|H\rangle_b|V\rangle_b|H\rangle_d|V\rangle_d,\tag{9a}$$

$$|\varphi\rangle_1 = \frac{1}{\sqrt{2}}(|H\rangle_a|H\rangle_b|H\rangle_d|V\rangle_d$$

$$- |V\rangle_a|V\rangle_b|H\rangle_d|V\rangle_d), \tag{9b}$$

$$|\varphi\rangle_2 = |H\rangle_a|V\rangle_a|H\rangle_d|V\rangle_d, \tag{9c}$$

$$|\varphi\rangle_3 = \frac{1}{\sqrt{2}}(|H\rangle_b|V\rangle_b|H\rangle_c|H\rangle_d - |H\rangle_b|V\rangle_b|V\rangle_c|V\rangle_d), \tag{9d}$$

$$|\varphi\rangle_4 = \frac{1}{2}(|H\rangle_a|H\rangle_b|H\rangle_c|H\rangle_d + |H\rangle_a|H\rangle_b|V\rangle_c|V\rangle_d + |V\rangle_a|V\rangle_b|H\rangle_c|H\rangle_d - |V\rangle_a|V\rangle_b|V\rangle_c|V\rangle_d), \tag{9e}$$

$$|\varphi\rangle_5 = \frac{1}{\sqrt{2}}(|H\rangle_a|V\rangle_a|H\rangle_c|H\rangle_d + |H\rangle_a|V\rangle_a|V\rangle_c|V\rangle_d), \tag{9f}$$

$$|\varphi\rangle_6 = |H\rangle_b|V\rangle_b|H\rangle_c|V\rangle_c, \tag{9g}$$

$$|\varphi\rangle_7 = \frac{1}{\sqrt{2}}(|H\rangle_a|H\rangle_b|H\rangle_c|V\rangle_c + |V\rangle_a|V\rangle_b|H\rangle_c|V\rangle_c, \tag{9h}$$

$$|\varphi\rangle_8 = |H\rangle_a|V\rangle_a|H\rangle_c|V\rangle_c, \tag{9i}$$

and the coefficients are

$$g_n = \pi^{-1/4}\,\mathrm{e}^{-(p-\sqrt{2}\alpha\sin n\theta)^2/2}, \tag{10}$$

$$\tau_n = \sqrt{2}\alpha\left(p - \frac{1}{\sqrt{2}}\sin n\theta\right)\cos n\theta, \tag{11}$$

$$N = (g_0^2 + 2g_1^2 + g_2^2 + 2g_3^2 + 4g_4^2 + 2g_5^2 + g_6^2 + 2g_7^2 + g_8^2)^{-1/2} \tag{12}$$

with $n = 0, 1, 2, \ldots, 8$.

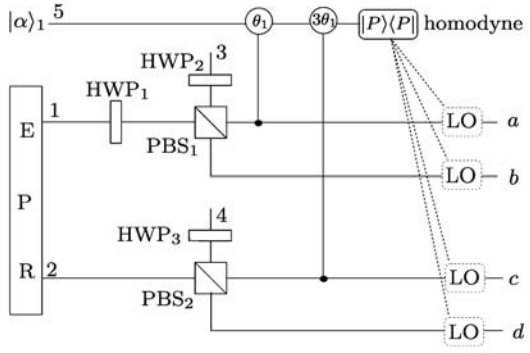


Fig. 1. The schematic diagram of Section 2. EPR denotes the entangled two-photon state $\frac{1}{2}(|H\rangle_1|H\rangle_2 + |V\rangle_1|V\rangle_2)$. PBS_1 and PBS_2 denote polarization beam splitters, which transmit the horizontal polarization and reflect the vertical one. HWP_1, HWP_2, and HWP_3 denote the half-wave plates, which implement transformation $|H\rangle \to (|H\rangle + |V\rangle)/\sqrt{2}$, $|V\rangle \to (|H\rangle - |V\rangle)/\sqrt{2}$; $|\alpha\rangle_1$ is the ancillary coherent state. The θ_1 ($3\theta_1$) indicates that the coherent beam will pick up a phase shift θ_1 ($3\theta_1$) when there is a photon in mode a (c), the dotted lines denote classical feedforward, LO denotes phase shift operation.

As a function of the homodyne measurement result p, $g_0, \sqrt{2}g_1, \ldots, g_8$ were plotted in Fig. 2. We observe that g_n are Gaussian curves with the peaks located at $\sqrt{2}\alpha\sin(n\theta)$. The distances between neighboring peaks are $2d_n = \sqrt{2}\alpha\{\sin(n\theta) - \sin[(n-1)\theta]\}$, which are referred to as the distinguishabilities of the measurement.[24] Since the distinguishabilities are approximately in proportion to $\alpha\theta$ when $\theta \ll 1$, we can use a strong coherent state probe light to ensure good distinguishability which makes the overlaps between these curves very small. Suppose the distinguishability of the measurement keeps the same, as long as the probe beam has a sufficient amplitude α, we can work with much smaller phase shifts; this property makes the protocol much easier to implement in practice. According to the measurement result p, simple local rotations using phase shifters can be performed via a feed-forward process to remove the relative phase τ_n. After the measurement, suppose the result is $400\sqrt{2}\sin 0.04 - \delta_1$, the corresponding fidelity is

$$F_{|\varphi_4\rangle}(400\sqrt{2}\sin 0.04 - \delta_1) = |\langle\varphi_4|\Psi\rangle_p|^2 \approx \frac{1}{1 + \frac{1}{2}\,\mathrm{e}^{-4d_4(d_4-\delta_1)}}, \tag{13}$$

which will be 0.9999 when $\delta_1 \approx 0.734d_4$. Besides, if the result is $400\sqrt{2}\sin 0.04 + \delta_2$ the corresponding fidelity is

$$F_{|\varphi_4\rangle}(400\sqrt{2}\sin 0.04 + \delta_2) = |\langle\varphi_4|\Psi\rangle_p|^2 \approx \frac{1}{1 + \frac{1}{2}\,\mathrm{e}^{-4d_5(d_5-\delta_2)}}, \tag{14}$$

when $\delta_2 \approx 0.733d_5$, this fidelity will be 0.9999, then, on condition that the fidelity is more than 0.9999, the probability to achieve the four-photon polarization-entangled cluster state $|\varphi\rangle_4$ is

$$P_4 = \int_{400\sqrt{2}\sin 0.04-\delta_1}^{400\sqrt{2}\sin 0.04+\delta_2} \langle p|\mathrm{Tr}_{\mathrm{signal}}(|\Psi\rangle_1\langle\Psi|)|p\rangle \mathrm{d}p \approx \frac{1}{8}[\mathrm{erf}(\delta_1) + \mathrm{erf}(\delta_2)], \tag{15}$$

where erf(x) is the error function, $\delta_1 \approx 0.734d_4$, $\delta_2 \approx 0.733d_5$. As the distinguishability of the measurement increases, the probability of obtaining the cluster state $|\varphi\rangle_4$ will approach 1/4.

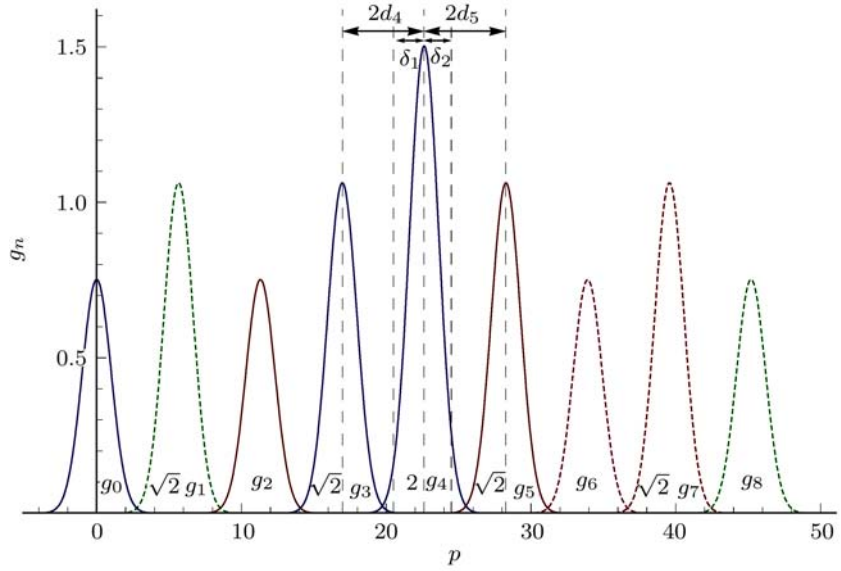


Fig. 2. (colour online) Curves of the homodyne measurement result p with $\alpha = 400$ and $\theta_1 = 0.01$.

Similar analysis can be made when the measurement result p is near the centers of the other eight side peaks in Fig. 2; the probability of obtaining $|\varphi\rangle_0$, $|\varphi\rangle_2$, $|\varphi\rangle_6$, $|\varphi\rangle_8$ will approach 1/16 and the probability of obtaining $|\varphi\rangle_1$, $|\varphi\rangle_3$, $|\varphi\rangle_5$, $|\varphi\rangle_7$ will approach 1/8 when the measurement distinguishability increases. Except $|\varphi\rangle_4$, the other states were thought to have failed in Ref. [15] but we can utilize some setups to translate these states into a four-photon polarization-entangled cluster state under a certain probability; we will explain it in Section 3 in detail.

3. Improvement of the success probability

Before starting in this section, we first introduce the setup described in Fig. 3. By employing some optical elements and weak cross-Kerr nonlinearity, the device in Fig. 3 could implement the following transformation

$$|H\rangle_{e_1}|V\rangle_{e_1}|\alpha\rangle_2 \to \frac{1}{2}[(|H\rangle_{f_1}|H\rangle_{f_2} - |V\rangle_{f_1}|V\rangle_{f_2})|\alpha\,\mathrm{e}^{3\mathrm{i}\theta_2}\rangle_2 + |H\rangle_{f_2}|V\rangle_{f_2}|\alpha\,\mathrm{e}^{4\mathrm{i}\theta_2}\rangle_2 - |V\rangle_{f_1}|H\rangle_{f_1}\rangle|\alpha\,\mathrm{e}^{2\mathrm{i}\theta_2}\rangle_2], \quad (16)$$

and

$$\begin{aligned}
&|H\rangle_{e_1}|V\rangle_{e_1}|H\rangle_{e_2}|V\rangle_{e_2}|\alpha\rangle_2|\alpha\rangle_3\\
\to\ &\frac{1}{4}[(|H\rangle_{f_1}|H\rangle_{f_2}|H\rangle_{f_3}|H\rangle_{f_4} - |H\rangle_{f_1}|H\rangle_{f_2}|V\rangle_{f_3}|V\rangle_{f_4}\\
&- |V\rangle_{f_1}|V\rangle_{f_2}|H\rangle_{f_3}|H\rangle_{f_4} + |V\rangle_{f_1}|V\rangle_{f_2}|V\rangle_{f_3}|V\rangle_{f_4})|\alpha\,\mathrm{e}^{3\mathrm{i}\theta_2}\rangle_2|\alpha\,\mathrm{e}^{3\mathrm{i}\theta_2}\rangle_3\\
&+ (|H\rangle_{f_1}|H\rangle_{f_2} - |V\rangle_{f_1}|V\rangle_{f_2})|H\rangle_{f_4}|V\rangle_{f_4}|\alpha\,\mathrm{e}^{3\mathrm{i}\theta_2}\rangle_2|\alpha\,\mathrm{e}^{4\mathrm{i}\theta_2}\rangle_3\\
&- (|H\rangle_{f_1}|H\rangle_{f_2} - |V\rangle_{f_1}|V\rangle_{f_2})|V\rangle_{f_3}|H\rangle_{f_3}|\alpha\,\mathrm{e}^{3\mathrm{i}\theta_2}\rangle_2|\alpha\,\mathrm{e}^{2\mathrm{i}\theta_2}\rangle_3\\
&+ (|H\rangle_{f_3}|H\rangle_{f_4} - |V\rangle_{f_3}|V\rangle_{f_4})|H\rangle_{f_2}|V\rangle_{f_2}|\alpha\,\mathrm{e}^{4\mathrm{i}\theta_2}\rangle_2|\alpha\,\mathrm{e}^{3\mathrm{i}\theta_5}\rangle_3\\
&- (|H\rangle_{f_3}|H\rangle_{f_4} - |V\rangle_{f_3}|V\rangle_{f_4})|V\rangle_{f_1}|H\rangle_{f_1}|\alpha\,\mathrm{e}^{2\mathrm{i}\theta_2}\rangle_2|\alpha\,\mathrm{e}^{3\mathrm{i}\theta_2}\rangle_3\\
&+ |H\rangle_{f_2}|V\rangle_{f_2}|H\rangle_{f_4}|V\rangle_{f_4}|\alpha\,\mathrm{e}^{4\mathrm{i}\theta_2}\rangle_2|\alpha\,\mathrm{e}^{4\mathrm{i}\theta_2}\rangle_3 - |H\rangle_{f_2}|V\rangle_{f_2}|V\rangle_{f_3}|H\rangle_{f_3}|\alpha\,\mathrm{e}^{4\mathrm{i}\theta_2}\rangle_2|\alpha\,\mathrm{e}^{2\mathrm{i}\theta_2}\rangle_3\\
&- |V\rangle_{f_1}|H\rangle_{f_1}|H\rangle_{f_4}|V\rangle_{f_4}|\alpha\,\mathrm{e}^{2\mathrm{i}\theta_2}\rangle_2|\alpha\,\mathrm{e}^{4\mathrm{i}\theta_2}\rangle_3 + |V\rangle_{f_1}|H\rangle_{f_1}|V\rangle_{f_3}|H\rangle_{f_3}|\alpha\,\mathrm{e}^{2\mathrm{i}\theta_2}\rangle_2|\alpha\,\mathrm{e}^{2\mathrm{i}\theta_2}\rangle_3]. \quad (17)
\end{aligned}$$

The use of the setups in Fig. 3 is to change bunching ones into unbunching outcomes at a certain probability, that is to say, with the help of these setups, we could improve our protocol's success probability. Next, we list two specific examples to show how to deal with $|\varphi\rangle_0$, $|\varphi\rangle_1, \ldots |\varphi\rangle_8$ (except $|\varphi\rangle_4$) for improv-

ing the success probability.

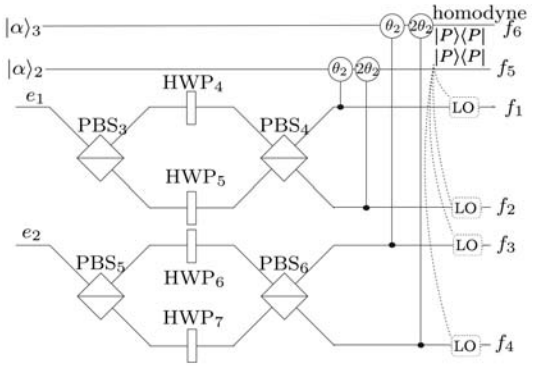


Fig. 3. The schematic plot of Section 3, PBS$_i$ ($i = 3, 4, 5, 6$) denote polarization beam splitters, HWP$_i$ ($i = 4, 5, 6, 7$) denote the half-wave plates, $|\alpha\rangle_2$ and $|\alpha\rangle_3$ are the ancillary coherent states respectively, the dotted lines denote classical feedforward, and LO denotes phase shift operation.

Example 1: After the operations in Section 2, if the output state is $|\varphi\rangle_7$, we let the spacial mode c pass through mode e_1 of the device in Fig. 3, and the state $\frac{1}{\sqrt{2}}(|H\rangle_a|H\rangle_b|H\rangle_{e_1}|V\rangle_{e_1} + |V\rangle_a|V\rangle_b|H\rangle_{e_1}|V\rangle_{e_1})$ will evolve into

$$\begin{aligned}|\varphi\rangle_9 = \frac{1}{2\sqrt{2}}[&(|H\rangle_a|H\rangle_b|H\rangle_{f_1}|H\rangle_{f_2}\\ &- |H\rangle_a|H\rangle_b|V\rangle_{f_1}|V\rangle_{f_2} + |V\rangle_a|V\rangle_b|H\rangle_{f_1}|H\rangle_{f_2}\\ &- |V\rangle_a|V\rangle_b|V\rangle_{f_1}|V\rangle_{f_2})|\alpha\,\mathrm{e}^{3\mathrm{i}\theta_2)}\rangle_2\\ &- (|H\rangle_a|H\rangle_b + |V\rangle_a|V\rangle_b)|V\rangle_{f_1}|H\rangle_{f_1}|\alpha\,\mathrm{e}^{2\mathrm{i}\theta_2}\rangle_2\\ &+ (|H\rangle_a|H\rangle_b + |V\rangle_a|V\rangle_b)|H\rangle_{f_2}|V\rangle_{f_2}|\alpha\,\mathrm{e}^{4\mathrm{i}\theta_2}\rangle_2],\end{aligned} \tag{18}$$

according to Eq. (16); Then we choose P-quadrature homodyne measurement on mode f_5, and the analysis of P-quadrature homodyne measurement is similar to that in Section 2, however, in this section we only consider the homodyne measurement in an ideal case (the error would be taken into account in Section 4). After the measurement, we have two kinds of results: (i) If the phase shift on coherent $|\alpha\rangle_3$ is $3\theta_2$, then equation (18) evolves into

$$\begin{aligned}|\varphi\rangle_{10} = \frac{1}{2}&(|H\rangle_a|H\rangle_b|H\rangle_{f_1}|H\rangle_{f_2}\\ &- |H\rangle_a|H\rangle_b|V\rangle_{f_1}|V\rangle_{f_2}\\ &+ |V\rangle_a|V\rangle_b|H\rangle_{f_1}|H\rangle_{f_2}\\ &- |V\rangle_a|V\rangle_b|V\rangle_{f_1}|V\rangle_{f_2}),\end{aligned} \tag{19}$$

which is similar to the cluster state in Eq. (1), but with a phase difference. We could utilize σ_z operation on spatial modes b and f_1 separately to achieve the cluster state that we want to generate. (ii) If the phase shift on the coherent state $|\alpha\rangle_2$ is $2\theta_2$ ($4\theta_2$), the corresponding state is $(|H\rangle_a|H\rangle_b + |V\rangle_a|V\rangle_b)|V\rangle_{f_1}|H\rangle_{f_1}$ $\big((|H\rangle_a|H\rangle_b + |V\rangle_a|V\rangle_b)|H\rangle_{f_2}|V\rangle_{f_2}\big)$, and we let the spatial mode f_1 (f_2) pass through the device in Fig. 3 again to transform the bunching state into an unbunching one with a probability 1/2, and then, with the help of σ_z operation, we can obtain the cluster state. Nevertheless, up to now, if we still achieve the bunching outcomes, the bunching state will be injected into the device in Fig. 3 again to gain the unbunching state. In a word, if we obtain an unbunching state, the protocol is successful; if we achieve the bunching state, we will let the state pass through the device again until we gain the unbunching state. In this case, after the operation in this section, the success probability is $P_1 = [1 - (1/2)^n]/8$ in an ideal condition, where n ($n = 0, 1, 2, 3, \ldots, +\infty$) is the iteration number of the bunching state. We use the same technique to deal with $|\varphi\rangle_1$, $|\varphi\rangle_3$, and $|\varphi\rangle_5$.

Example 2: If the output state is $|\varphi\rangle_8$ in Section 2, we let the spatial mode a and spatial modes c pass through the spatial modes e_1 and e_2 of the device in Fig. 3, and the evolution of the state $|H\rangle_{e_1}|V\rangle_{e_1}|H\rangle_{e_2}|V\rangle_{e_2}|\alpha\rangle_2|\alpha\rangle_3$ is shown as in Eq. (17); then we choose P-quadrature measurement on the spatial modes f_5 and f_6, and there are three kinds of results: i) If the phase shift on coherent $|\alpha\rangle_2$ and $|\alpha\rangle_3$, both equal to $3\theta_2$, then equation (17) evolves into

$$\begin{aligned}|\varphi\rangle_{11} = \frac{1}{2}&(|H\rangle_{f_1}|H\rangle_{f_2}|H\rangle_{f_3}|H\rangle_{f_4}\\ &- |H\rangle_{f_1}|H\rangle_{f_2}|V\rangle_{f_3}|V\rangle_{f_4}\\ &- |V\rangle_{f_1}|V\rangle_{f_2}|H\rangle_{f_3}|H\rangle_{f_4}\\ &+ |V\rangle_{f_1}|V\rangle_{f_2}|V\rangle_{f_3}|V\rangle_{f_4}),\end{aligned} \tag{20}$$

with the help of unitary operation, we can translate Eq. (20) to the cluster state. ii) If the phase shifts on coherent $|\alpha\rangle_2$ and $|\alpha\rangle_3$ equal $3\theta_2$ and $4\theta_2$ ($3\theta_2$ and $2\theta_2$; $4\theta_2$ and $3\theta_2$; $2\theta_2$ and $3\theta_2$) respectively, the corresponding state is $(|H\rangle_{f_1}|H\rangle_{f_2} - |V\rangle_{f_1}|V\rangle_{f_2})|H\rangle_{f_4}|V\rangle_{f_4}$ $\big((|H\rangle_{f_1}|H\rangle_{f_2} - |V\rangle_{f_1}|V\rangle_{f_2})|V\rangle_{f_3}|H\rangle_{f_3}$; $(|H\rangle_{f_3}|H\rangle_{f_4} - |V\rangle_{f_3}|V\rangle_{f_4})|H\rangle_{f_2}|V\rangle_{f_2}$; $(|H\rangle_{f_3}|H\rangle_{f_4} - |V\rangle_{f_3}|V\rangle_{f_4})$ $|V\rangle_{f_1}|H\rangle_{f_1}\big)$, the way to deal with these states is similar to Example 1. iii) If the phase shifts on coherent $|\alpha\rangle_2$ and $|\alpha\rangle_3$ equal $4\theta_2$ and $4\theta_2$ ($4\theta_2$ and $2\theta_2$; $2\theta_2$ and $4\theta_2$; $2\theta_2$ and $2\theta_2$) respectively, the corresponding state is $|H\rangle_{f_2}|V\rangle_{f_2}|H\rangle_{f_4}|V\rangle_{f_4}$ $\big(|H\rangle_{f_2}|V\rangle_{f_2}|V\rangle_{f_3}|H\rangle_{f_3}$; $|H\rangle_{f_1}|V\rangle_{f_1}|V\rangle_{f_4}|H\rangle_{f_4}$; $|V\rangle_{f_1}|H\rangle_{f_1}|V\rangle_{f_3}|H\rangle_{f_3}\big)$. We

will repeat the earlier work in Example 2, and these states would be injected into the setup in Fig. 3 again to gain the unbunching states. After these operations, the success probability of Example 2 is

$$P_2 = \frac{1}{16}\left(1 + \frac{1}{4^n} - \frac{1}{2^{n-1}}\right) = \frac{4^n - 2^{n+1} + 1}{4^{n+2}}$$

in an ideal condition, where n ($n = 0, 1, 2, 3, \ldots, +\infty$) is the iteration number of the bunching state. The technique to deal with $|\varphi\rangle_0$, $|\varphi\rangle_2$, and $|\varphi\rangle_6$ is the same as with $|\varphi\rangle_8$.

4. Discussion and conclusion

So far, we have enumerated different countermeasures to handle every outcome state in Section 2 in order to achieve the cluster state. The success probability of our protocol depends mainly on the precision of the homodyne measurement. We suppose the accurate rate of the homodyne measurement is η in each iteration operation. The total success probability of our protocol is

$$P_{\text{total}} = \frac{1}{4}\eta + \frac{\eta^2[1-(\eta/4)^n]}{2-\eta} - \frac{3\eta[1-(\eta/4)^n]}{16-4\eta}. \quad (21)$$

From Fig. 4, we can see that the overall success probability P_{total} increases when increasing the iteration number n and the accurate rate of the homodyne measurement η. Analysis of the accurate rate in the momentum quadrature homodyne measurement is presented in Ref. [25], the author verified that as long as $\alpha\theta \sim \pi$ the overlap error is smaller than 10^{-3}; in other words, the accuracy of the homodyne measurement η is more than 0.999 on condition that $\alpha\theta \sim \pi$. Recently, with the help of electromagnetically induced transparency(EIT), the nonlinearities might be largely improved, say $\theta \sim 10^{-2}$,[26−30] therefore, a probe coherent state $|\alpha\rangle$ with an amplitude $\alpha = 300$ will implement our protocol well in practice. With regard to the practical implementation of our protocol, another important factor is that the decoherence effects during the entanglement generation process in nonlinear media must be low.[31] We can gain further information from Fig. 4, when iteration number $n \geq 4$, the success probability increases slowly but more and more operations are needed, thus, iterating too many times is not good for our protocol.

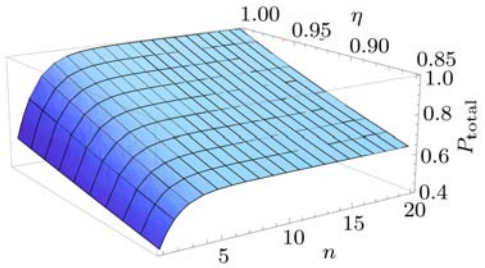


Fig. 4. (colour online) The total success probability P_{total} versus n and η.

In summary, we have presented an effective protocol to generate a four-photon polarization-entangled cluster state by using linear optical elements and cross-Kerr nonlinearity. In contrast to the previous scheme,[32−34] our protocol has a higher success probability, and we can predict that our protocol is successful or not from the momentum homodyne measurements without destroying the output states. Furthermore, our protocol provides an alternative method to improve success probability for the protocols which require that the outcome states are unbunching ones. The protocol uses only the basic tools in quantum optical laboratories and can be implemented using the current techniques.

References

[1] Einstein A, Podolsky B and Rosen N 1935 *Phys. Rev.* **47** 777
[2] Ekert A K 1991 *Phys. Rev. Lett.* **67** 661
[3] Bennett C H and Wiesner S J 1992 *Phys. Rev. Lett.* **69** 2881
[4] Bennett C H, Brassard G, Crepeau C, Jozsa R, Peres A and Wootters W K 1993 *Phy. Rev. Lett.* **70** 1895
[5] Briegel H J and Raussendorf R 2001 *Phys. Rev. Lett.* **86** 910
[6] Nielsen M A 2004 *Phys. Rev. Lett.* **93** 040503
[7] Raussendorf R and Briegel H J 2001 *Phys. Rev. Lett.* **86** 5188
[8] Dür and Briegel H J 2004 *Phys. Rev. Lett.* **92** 180403
[9] Raussendorf R and Briegel H J 2001 *Phys. Rev. Lett.* **86** 5188
[10] Zhou D L, Zeng B, Xu Z and Sun C P 2003 *Phys. Rev.* A **68** 062303
[11] Raussendorf R, Browne D E and Briegel H J 2003 *Phys. Rev.* A **68** 022312
[12] Nielsen M A 2004 *Phys. Rev. Lett.* **93**, 040503
[13] Nielsen M A and Dawson C M 2005 *Phys. Rev.* A **71** 042323
[14] Chen J L, Xue K and Ge M L 2007 *Phys. Rev.* A **76** 042324
[15] Zou X B and Mathis W 2005 *Phys. Rev.* A **71** 032308
[16] Imoto N, Haus H A and Yamamoto Y 1985 *Phys. Rev.* A **32** 2287
[17] Nemoto K and Munro W J 2004 *Phys. Rev. Lett.* **93** 250502

[18] Munro W J, Nemoto K, Beausoleil R G and Spiller T P 2005 *Phys. Rev.* A **71** 033819
[19] Guo Q, Bai J, Cheng L Y, Shao X Q, Wang H F and Zhang S 2011 *Phys. Rev.* A **83** 054303
[20] Xia Y, Song J, Lu P M and Song H S 2011 *J. Phys.* B: *At. Mol. Opt. Phys.* **44** 025503
[21] Hinkley E D and Freed C 1963 *Phys. Rev. Lett.* **23** 277
[22] Jiang L A and Luu J X 2008 *Appl. Opt.* **47** 1486
[23] Zhao C R and Ye L 2011 *Opt. Commun.* **284** 541
[24] Ladd T D, Van L P and Nemoto K 2006 *New J. Phys.* **8** 184
[25] Louis S G R, Nemoto K, Munro W J and Spiller T P 2007 *New J. Phys.* **9** 193
[26] Schmidt H and Imamoğlu A 1996 *Opt. Lett.* **21** 1936
[27] Lukin M D and Imamoğlu A 2000 *Phys. Rev. Lett.* **84** 1419
[28] Lukin M D and Imamoğlu A 2001 *Nature* **413** 273
[29] Munro W J, Nemoto K, Beausoleil R G and Spiller T P 2005 *Phys. Rev.* A **71** 033819
[30] Jin G S, Lin Y and Wu B 2007 *Phys. Rev.* A **75** 054302
[31] Jeong H 2005 *Phys. Rev.* A **72** 034305
[32] Zhao C R and Ye L 2011 *Sci. China.* (*Phys. Mech. Astron.*) **54** 479
[33] Du Q H, Ye M Y, Chen Z H, Li X H and Lin X M 2008 *Commun. Theor. Phys.* **50** 623
[34] Lai B H, Du G, Yu Y F, Zhang Z M and Liu S H 2010 *Acta Phys. Sin.* **59** 1017 (in Chinese)